Journal of Fluorescence (2020) 30:317–327
https://doi.org/10.1007/s10895-020-02503-4

ORIGINAL ARTICLE

Fluorescence "Turn On–Off" Sensing of Copper (II) Ions Utilizing Coumarin–Based Chemosensor: Experimental Study, Theoretical Calculation, Mineral and Drinking Water Analysis

Fatma Nur Arslan[1,2] · Gonul Akin Geyik[1] · Kenan Koran[3] · Furkan Ozen[4] · Duygu Aydin[1] · Şükriye Nihan Karuk Elmas[1] · Ahmet Orhan Gorgulu[3] · Ibrahim Yilmaz[1]

Received: 13 January 2020 / Accepted: 27 January 2020 / Published online: 3 February 2020
© Springer Science+Business Media, LLC, part of Springer Nature 2020

Abstract

Herein, we report the preparation of a fluorescent sensor based on coumarin derivative for copper (II) ion sensing in CH_3CN/HEPES media. 6,7–dihydroxy–3–(4–(trifluoro)methylphenyl)coumarin (**HMAC**) sensor was fabricated and analyzed by spectroscopic techniques. The sensor demonstrates "turn on–off" fluorescence quenching in the presence of copper (II) ions at 458 nm. A clear complex between the chemosensor **HMAC** and copper (II) ions was characterized by ESI–MS as well as the Job's method. Also, the limit of detection (LOD, $3\sigma/k$) value was determined as 24.5 nM in CH_3CN/HEPES (95/5, *v*/v) buffer media (pH = 7.0). This value is lower than the admissible level of copper (II) ions in drinking water (maximum 31.5 μM) reported by EU Water Framework Directive (WFD) and World Health Organization (WHO) guidelines. The theoretical calculations (density functional theory, DFT) have been performed for the geometric optimized structures. As a final stage, real sample analyses have successfully been performed by using **HMAC**, as well as ICP–OES method. The relative standard deviation for copper (II) in mineral and drinking water samples has been determined to be below 0.15% and recovery values are in the range of 95.48–109.20%.

Keywords Fluorescence sensor · Copper · Coumarin · Drinking water · Mineral water · DFT

Introduction

Copper ion is the most abundant d–block metal ion in the human body behind iron and zinc ions. It is a crucial agent in many fundamental physiological and biological processes, for instance, mitochondrial electron transport, enzyme functions, producing red blood cells, acting as a catalyst for the production of melanin, and also serving to be neurotransmitters [1–3]. The

Electronic supplementary material The online version of this article (https://doi.org/10.1007/s10895-020-02503-4) contains supplementary material, which is available to authorized users.

✉ Ibrahim Yilmaz
iyilmaz@kmu.edu.tr

Fatma Nur Arslan
arslanfatmanur@gmail.com

Gonul Akin Geyik
gnlakin@gmail.com

Kenan Koran
kenan.koran@gmail.com

Furkan Ozen
furkanozen@akdeniz.edu.tr

Duygu Aydin
duyguaydin@kmu.edu.tr

Şükriye Nihan Karuk Elmas
snihankaruk@gmail.com

Ahmet Orhan Gorgulu
aogorgulu@firat.edu.tr

[1] Department of Chemistry, Kamil Ozdag Science Faculty, Karamanoglu Mehmetbey University, 70100 Karaman, Turkey

[2] Van't Hoff Institute for Molecular Sciences, Analytical–Chemistry Group, University of Amsterdam, Amsterdam, Netherlands

[3] Department of Chemistry, Firat University, Science Faculty, 23119 Elazıg, Turkey

[4] Department of Mathematics and Science, Akdeniz University, Faculty of Education, 07058 Antalya, Turkey

human body may intake copper ions through food, drinking water, environmental and biological sources, as well as through skin contact to copper containing compounds. However, maintaining the copper level within a particular range below toxic concentrations is a challenge [4–6]. It is well known that high level of copper ions in human body causes the disturbance of cellular homeostasis leading to oxidative stress and disorders such as brain and neurodegenerative diseases such as Parkinson's and Alzheimer's diseases, and also leads to liver or kidney damages [1–10]. For drinking water samples, the maximum admissible level of copper ions is 2 $mg.L^{-1}$ according to the WHO and EU–WFD [4, 6–10]. Since copper ions can accumulate into the human body through drinking water, the detection of its levels in mineral or drinking water samples is vital to control its impact on the human health.

Although a wide range of traditional methodologies for example inductively coupled mass atomic emission spectrometry (ICM–AES) [11], plasmon resonance sensor [12], graphite flame atomic absorption spectrometry (AAS) [4, 13], electrochemical assays [14], Rayleigh scattering spectroscopy (RSS, plasmon–resonance) [15], inductively coupled plasma optical emission spectroscopy (ICP–OES) [16], and etc. have been employed to monitor copper (II) ions, as a consequence, fluorescence chemosensors based techniques remain attractive, because of their high efficiency, operational simplicity, sensitive detection and non–destructiveness [1, 2, 4–7, 9, 10, 17]. Recently, thousands of investigations have been placed on the development of novel, highly selective and sensitive fluorescent chemosensors for the determination of copper ions [18–27]. For this purpose, various organic molecules such as rhodamine, BODIPY, coumarin, fluorescein and cyanine are widely used to monitor copper (II) ions in different media [20]. Among these organic molecules, fluorescent sensors based on coumarin derivative in the literature offer the selective and sensitive monitoring of copper (II) ions as well as high accuracy. However, the studies based on the fluorescent chemosensor based on coumarin derivative for copper (II) monitoring in real drinking and water samples are quite limited. For example, a fluorescent chemosensor based on coumarin derivative for the efficient monitoring of copper (II) ions in wine samples was successfully developed by Wu and coworkers [28], and the limit of detection was found as 62 nM. In another study, Yan and coworkers designed a novel FRET ratiometric sensor for the monitoring of copper (II) ion in tap and lake water samples with satisfactory recovery ratios, and the limit of detection was found as 210 nM [29]. Duan and coworkers presented a novel fluorescent chemosensor based on coumarin derivative for sensing copper (II) ion present in deionized water samples. The detection limit was measured to be 52 nM [30]. However, detection limits in the mentioned studies are still above the legal acceptance values reported by WHO and EU–WFD guidelines for drinking water samples (31.5 μM). Hence, the fabrication of novel fluorescent chemosensors based on coumarin derivatives for copper (II) ion sensing with high accuracy and recovery values is noticeably urgent.

In an effort to contribute towards the above issues, a new 6,7–dihydroxy–3–(4–(trifluoro)methylphenyl)coumarin (**HMAC**) sensor based molecular system is fabricated for the sensitive and selective sensing of copper (II) ions. Coumarin has been employed to be a fluorophore due to its high fluorescence quantum yield, high chemical stability, large Stoke's shift and moderately high water solubility. Besides, coumarin derivatives are less toxic to environment and the livings [31–33]. Herein, we reported the preparation of a fluorescent "turn on–off" chemosensor based on coumarin derivative for copper (II) monitoring in mineral and drinking waters with a quite simple operation. Firstly, **HMAC** fluorescent sensor was synthesized and then successfully characterized by ^{13}C–NMR, ^{1}H–NMR and FT–IR techniques. Afterwards, it was evaluated for the selective determination of copper (II) ions in CH_3CN/HEPES media (95/5, *v*/v) at pH = 7.0. The theoretical calculations, DFT, were also carried out for the geometric optimized structures. In the last part of study, the sensor **HMAC** was applied for the various real mineral and drinking water samples. Fabricated sensor **HMAC** presents low detection limits and shows a good performance for a series of mineral and drinking water.

Materials and Methods

Chemicals and Instruments

All chemicals were of analytical reagent grade and purchased from VWR international (Poole, UK), Sigma–Aldrich (Lyon, France) and Merck (Darmstadt, Germany) chemical companies. Perchlorate salts of different metal ions (Cu^{2+}, Zn^{2+}, Cd^{2+}, Ca^{2+}, Sr^{2+}, Ba^{2+}, Mg^{2+}, Mn^{2+}, Fe^{2+}, Fe^{3+}, Co^{2+}, Na^{+}, Hg^{2+}, $Pb^{2+}$and Al^{3+}) were used. Ultrapure water was supplied by Millipore water purification system (Millipore Corp., Billerica, MA). ^{1}H and ^{13}C NMR spectra were obtained on a Bruker DPX 400 MHz spectrometer. A spectrum 100 FT–IR spectrometer (Perkin Elmer Inc., Wellesley, MA) was employed to measure the FT–IR spectra of compounds. Fluorescence spectra were recorded on a Varian Cary Eclipse fluorescence spectrophotometer (Agilent Technologies Inc., Santa Clara, CA, USA). A mass spectrum was obtained on a Bruker Mass Spectrometer (Daltonics Microflex) equipped with an ESI source. An inductively coupled plasma–optical emission spectroscopy (ICP–OES, Agilent 720) system (Agilent Technologies, Wilmington, USA) equipped with an axial plasma torch was used.

Preparation of the Chemosensor HMAC

The compounds 6,7–dihydroxy–3–(3–methylphenyl)coumarin **(**probe **HMAC)** and 2–(2,4,5–trimethoxyphenyl)–1–(3–(methylphenyl))acrylonitrile **(HMAN)** were fabricated and purified according to the literature [17, 34, 35]. The procedures are given in supporting information file.

Fluorescence Studies of Probe HMAC

The stock solution of **HMAC** (10 mM) was prepared in CH_3CN and diluted to appropriate concentration (5.0 μM). The emission intensities of the probe **HMAC** system (5.0 μM) were performed in CH_3CN/HEPES (95/5, *v*/v) at pH = 7.0 buffer media, and the excitation wavelength was 364 nm. 1.10^{-3} M of perchlorate salts of the metal ions was prepared in ultrapure water. The excitation and emission wavelengths were adjusted as 364 nm and 458 nm (slit width 5 nm), respectively.

The fluorescence titration experiments were carried out triplicate at 458 nm, and the LOD value of the chemosensor **HMAC** was calculated using the $3\sigma/k$ equation. (σ = standard deviation of blank solution, k = the slope of the calibration curve between the amount of copper (II) and fluorescence intensity of chemosensor **HMAC**). The interference behaviours were tested by excitation at 364 nm, in the presence of various metal ions [10–fold excess solutions, $M(ClO_4)_nxH_2O$)] and copper (II) ion.

Theoretical DFT Calculation

The calculations were performed using the Gaussian 09 software (Gaussian, Inc., Wallingford CT) with B3LYP and 6–31 g(d) basis sets [36–40]. The theoretical calculations were carried out for the geometrically optimized structures, the energy levels (HOMO and LUMO) of the probe **HMAC** and complex of the **HMAC–Cu^{2+}**.

Sensing of Copper (II) Ions in Real Samples

To demonstrate the applicability of the probe **HMAC** in real samples, various mineral and drinking water samples were analyzed. Samples were obtained from local markets (Karaman city, Turkey). As an initial step, the waters were degassed to remove the carbonate present in the samples; and then they were put on an ultrasonic bath and sonicated for 15 min. Afterwards, tested samples were centrifuged at 8.000 rpm for 10 min, and then filtered using a 0.45.0 μM pore–size membrane filter to get rid of suspended species or contamination.

Procedure of Copper (II) Ion Determination by Fluorescence Spectroscopy

Following the centrifugation and filtration procedures, the spectroscopic measurements were carried out by the following procedure. Briefly, 5.0 μM of ligand (probe **HMAC**) solution was freshly prepared in 95/5, *v*/v, CH_3CN/HEPES buffer media (pH = 7.0) before analysis. For each experiment, 3 mL of the ligand solution was added to fluorescence cuvette and spectra were recorded. Then, 15 μL of real sample was added to this solution and it was mixed for a few seconds. Fluorescence spectra of the mixed solution (probe **HMAC** + real sample) were taken again at room temperature (λ_{exc} = 364 nm, λ_{emm} = 458 nm with 5 nm of slit size). Also, to evaluate the method accuracy, standard addition method was performed by adding 15 μL of copper (II) solutions (0.1 μM and 0.2 μM) into the mixed solution.

Procedure of Copper (II) Ion Determination by ICP–OES

Before the ICP–OES analyses, the pre–treatment procedure for real samples was done according to the method proposed by Mendil et al. [41]. Briefly, the mineral and drinking water samples were acidified with 1% of nitric acid and the solutions were adjusted to pH = 9 by NH_3/NH_4Cl buffer solution. They were kept approximately 10 min and then the solutions were centrifuged at 8.000 rpm for 15 min. The upper layers were suspended and the precipitates were dissolved with 0.5 mL of concentrated nicric acid. Finally, the samples were diluted to 2.5 mL of HPLC grade water and analyzed by ICP–OES in triplicate. The operating parameters of system were given in **Table S1**. The measurement results were reported as mean value ±SD.

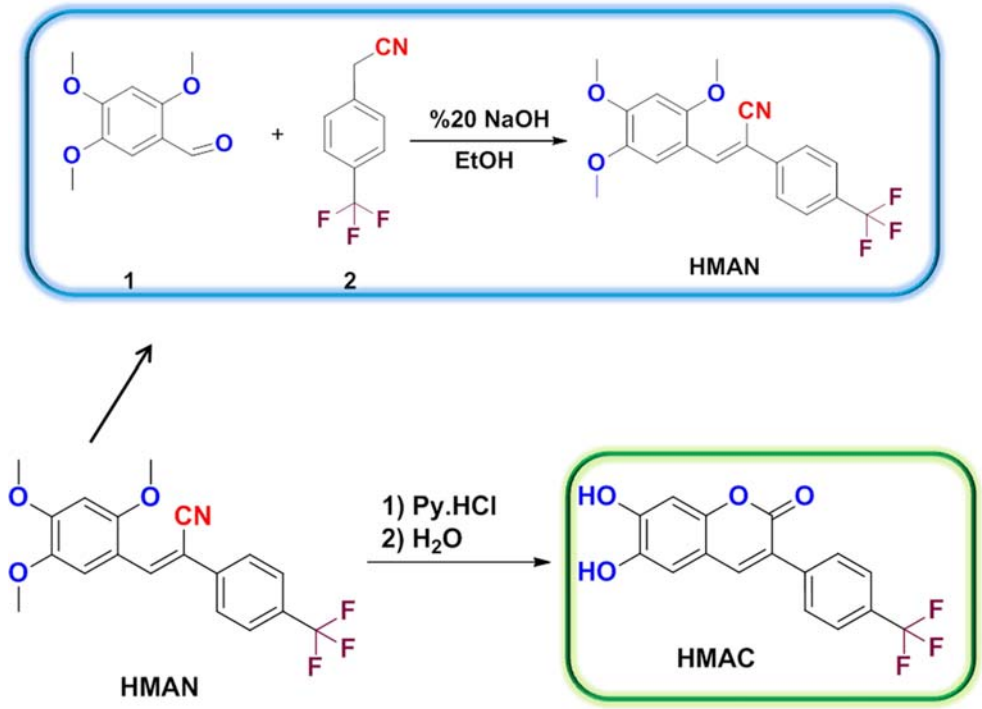
Results and Discussion

Fabrication and Characterization of HMAN and Probe HMAC

Synthesis and purification of **HMAN** were done according to previous literatures [17, 34, 35]. After filtering the synthesized phenylacrylonitrile compound, it was washed with ultrapure water until the neutral pH. **HMAC** was synthesized in a non–solvent silica gel condition under microwave irradiation at high yield in the presence of **HMAN** with pyridinium hydrochloride, and column chromatography was chosen to purify the crude product. The general procedure for synthesis is presented in Scheme 1.

Silica gel was used as a solid support for the synthesis step of **HMAC**. This support material reduced formation of side products and has been effective for obtaining the

Scheme 1 Synthetic scheme of **HMAN** and **HMAC**



main products with high yields. Pyridinium hydrochloride was used to transform hydroxyl groups of methoxy groups in the compound **HMAC**. Therefore, the lactone ring was formed and resulted in a changing from the hydroxyl groups to nitrile carbon. FT–IR, ^{1}H–, ^{13}C– and APT–NMR techniques were used to confirm the structure of synthesized compounds. When comparing the NMR and FT–IR spectra of **HMAN** and **HMAC**, it is easily seen that the –C ≡ N peaks of **HMAN** do not exist at spectrum of the compound **HMAC**. Also, the disappearance of methoxy and formation of –OH stretching vibrations are clearly monitored at 3190 and 3412 cm^{-1} in the **HMAC** spectrum. The lactone ring of the coumarin compound has specific –C=O stretching vibrations monitored at 1661 cm^{-1}. The disappearance of methoxy protons and formation of –OH proton peaks prove that there is a clear product formation. All of the characterization data is given in Fig. S1 to S7.

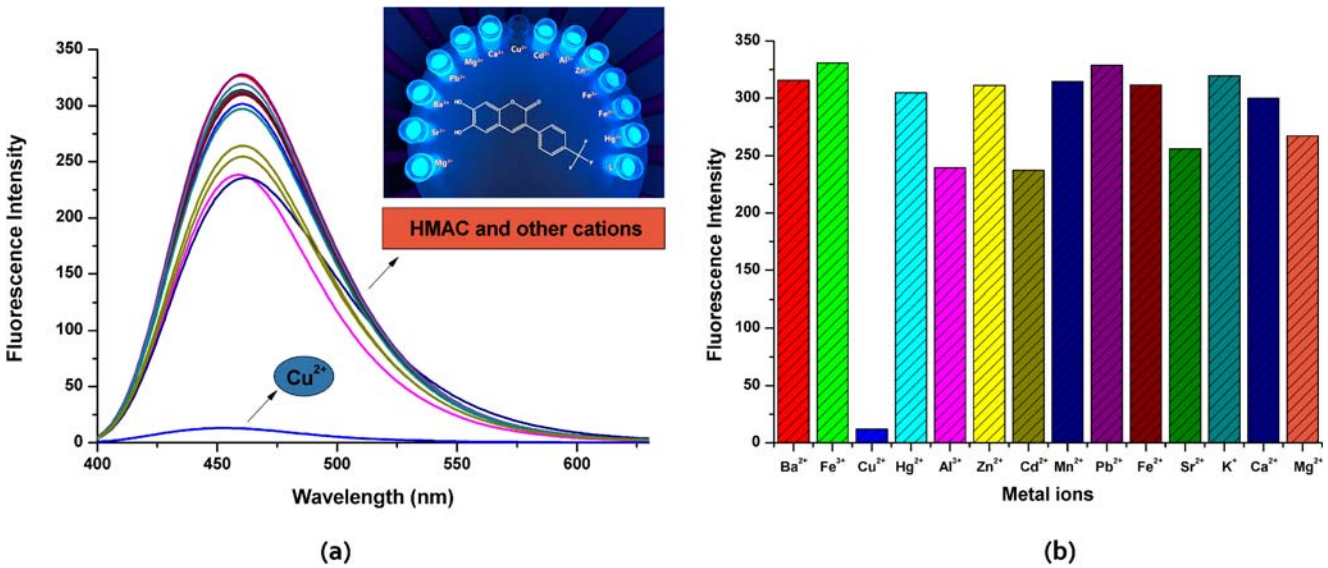


Fig. 1 **(a)** Fluorescence intensity changes of probe **HMAC** (5.0 μM) in the presence of various cations (50 μM) in ACN/HEPES buffer solution (95/5, *v*/v, pH = 7.0), **(b)** Changes in the fluorescence intensity ratio (I_o/I) of probe **HMAC** in the presence of various metal ions in ACN/HEPES buffer solution (95/5, v/v, pH = 7.0) (λ_{emm} = 458 nm, λ_{exc} = 364 nm)

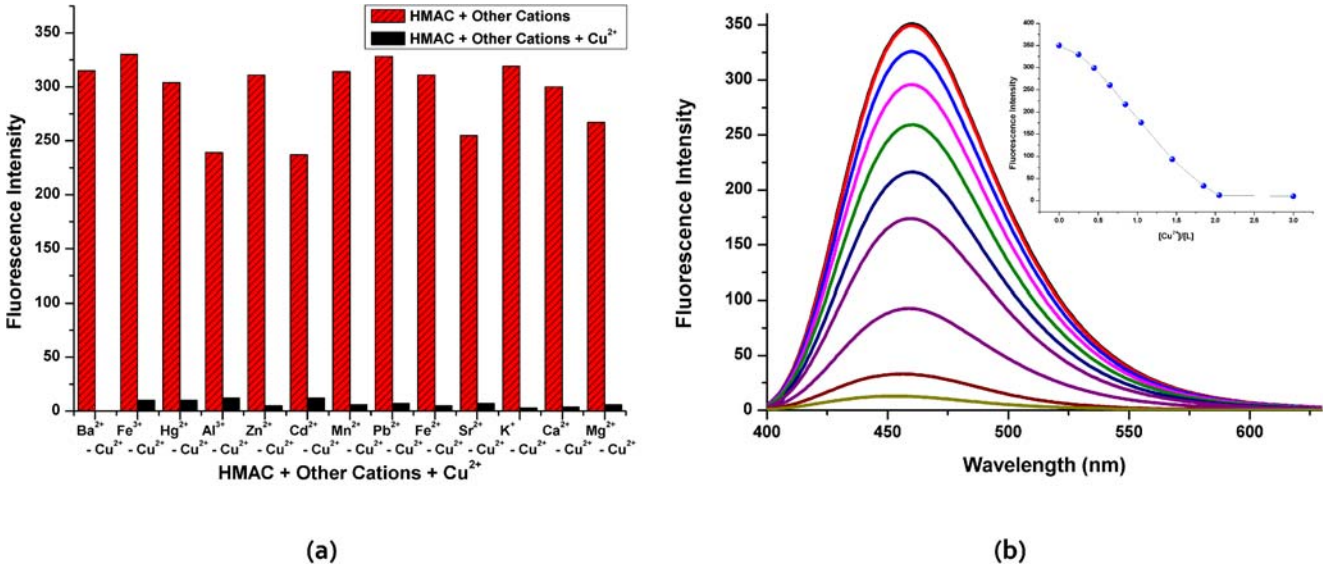
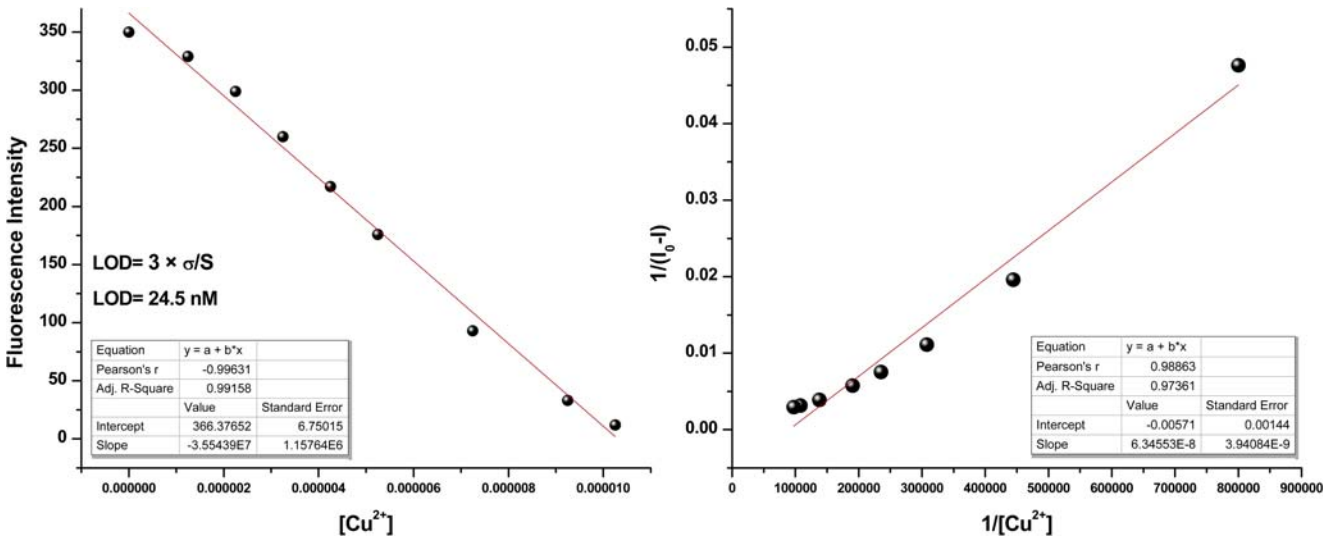


Fig. 2 **(a)** Selectivity of the **HMAC**–Cu^{2+} sensor over the different metal ions in ACN/HEPES buffer solution (95/5, v/v, 5.0 μM, pH = 7.0) **(b)** the fluorescence spectra of **HMAC** with the increasing concentrations of copper (II) in ACN/HEPES buffer solution (95/5, v/v, 5.0 μM, pH = 7.0) (λ_{emm} = 458 nm, λ_{exc} = 364 nm)

Fluorescence Studies

Selectivity is one of the most important performance parameters for fluorescent sensors. In this study, the ability of the chemosensor **HMAC** for the detection of copper (II) in the existence of 10–fold excess of various cations (Mg^{2+}, Mn^{2+}, Ca^{2+}, Sr^{2+}, Co^{2+}, Ba^{2+}, Fe^{2+}, Hg^{2+}, Cu^{2+}, Zn^{2+}, Fe^{2+}, Pb^{2+}, Cd^{2+}, Al^{3+} and Na^{+}) was evaluated. As shown in Fig. 1, when these ions were added into the **HMAC** solution, only copper (II) ions result in a significant fluorescence quenching at 458 nm. None of the other metal cations generated obvious impact on fluorescence intensities. In addition to fluorescence emission study, UV–Visible experiments were performed, and obtained results were presented in **Fig. S8**. In the presence of copper, an increase in the absorbance intensity of the sensor **HMAC** at 230 nm was observed, while the peak at 370 nm was shifted to 300 nm, in other words towards the blue wavelength. Thus, chemosensor **HMAC** demonstrated a high selectivity for copper (II) ions over tested metal ions.

To study the impact of the other metal cations on the recognition of probe **HMAC** system to copper (II) (10.0 eq.), each of the other metal cations (10.0 eq.) was added into the probe **HMAC**–copper (II) solution, respectively (Fig. 2a). The selectivity studies of probe **HMAC** (5.0 μM) were performed at 458 nm in CH_3CN/HEPES buffer media (95/5, *v*/v) at pH = 7.0. As depicted in Fig. 2a, the fluorescence emission



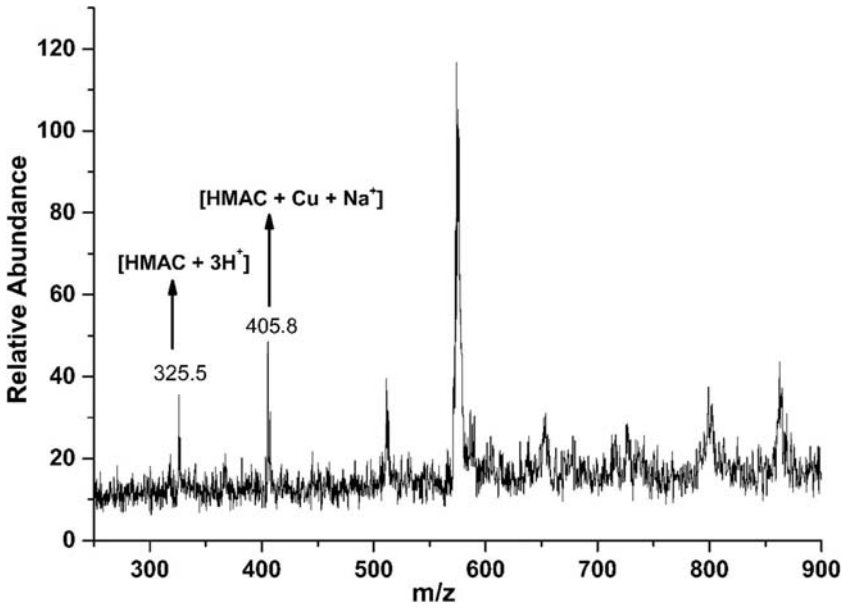


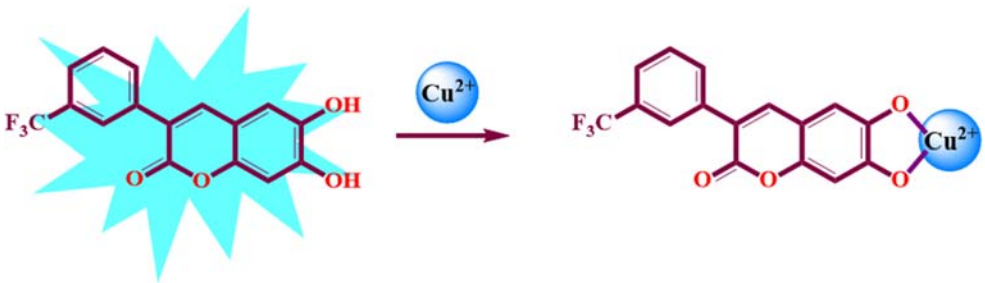
Fig. 4 ESI–MS spectrum of probe **HMAC**–Cu^{2+} complex

intensity of probe **HMAC**–copper (II) solution changed only a little when adding the tested cations, which proposed that the recognition process of copper (II) was scarcely influenced by tested cations. Consequently, probe **HMAC** system had high selectivity on monitoring copper (II) ion. To obtain quantitative relation of probe **HMAC** (5.0 μM) solution on sensing copper (II) ion, the fluorescence titration experiments in CH_3CN/HEPES buffer media (95/5, v/v) at pH = 7.0 were performed (Fig. 2b). As can be seen from Fig. 2b, the fluorescence emission intensity at 458 nm gradually decreased with the copper (II) concentration (0 to 50 μM) increased. After the addition of 2.0 equivalent of copper (II) ion, quenching of the fluorescence intensity reached a constant value. This quenching which resulted from the formation of the **HMAC**–Cu^{2+} complex, may be attributed to the paramagnetic effect and heavy atom effect of transition metals [42]. Hence, the probe **HMAC** could be employed as a "turn–on–off" fluorescent chemosensor for sensing copper (II) ions.

Based on the fluorescence titration experiments, the calibration curve of the quantitative correlation between the emission value and metal concentration was $y = -3.56 \times 10^7 x + 366.38$ ($R^2 = 0.9916$) (Fig. 3a). The detection limit of the chemosensor **HMAC** for copper (II) ion sensing was found to be 24.5 nM on the basis of $3\sigma/k$ and the linearity range was so extensive. The LOD value of probe **HMAC** enables the copper (II) ion monitoring in nanomolar levels, and therefore it is lower than the acceptable limit of the drinking water guidelines of WHO and EU–WFD (31.5 μM) [4, 6–10]. Furthermore, the correlation constant value was calculated to be 9.00×10^4 M^{-1} using the Benesi–Hildebrand equation based on the data of fluorescence titration (Fig. 3b). Thus, these results showed that the probe **HMAC** system had good sensitivity on copper (II), and the standard curve with good linearity ($R^2 = 0.9916$) could be used to quantify.

During detecting copper (II) ion with probe HMAC system as fluorescent probe, fluorescence quenching occurred, which meant copper (II) ion interacted with probe HMAC system. To investigate the structure of HMAC–Cu^{2+} complex, ESI–MS spectra were obtained (Fig. 4). The formation of a complex between HMAC–Cu^{2+} (Scheme 2) was verified by the ESI–MS technique. As can be seen from MS spectrum, the peak at m/z = 405.8 corresponds to the [HMAC+ Cu + Na^+] was indicated 1:1 ratio in Fig. 4.

Also, to detect the stoichiometric ratio of copper (II) ion and probe HMAC in HMAC–Cu^{2+} complex, Job's graph was plotted based on fluorescence titration data (Fig. 5). As shown



Scheme 2 The proposed binding mechanism of probe **HMAC** and copper (II) complex in ACN/HEPES buffer solution (95/5, v/v, 5.0 μM, pH = 7.0)

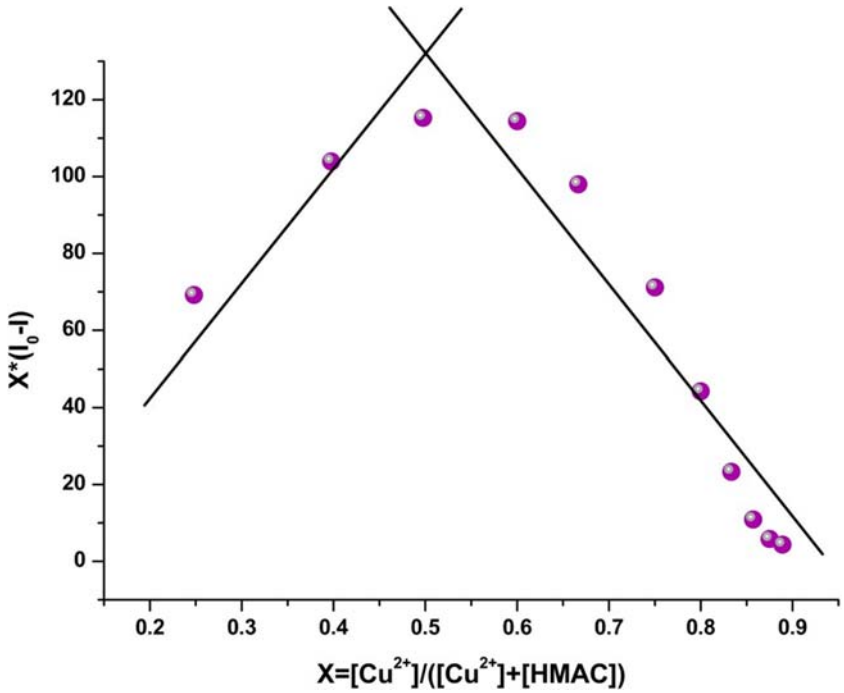


Fig. 5 Job plots of **HMAC**–Cu^{2+} complex in ACN/HEPES buffer solution (95/5, v/v, 5.0 μM, pH = 7.0) (λ_{emm} = 458 nm, λ_{exc} = 364 nm)

in Fig. 5, the stoichiometry of the HMAC–Cu^{2+} complex was found to be 1:1 ratio, due to the maximum of relative intensity was about 0.5 value.

The response time of the probe **HMAC** were also performed for real–time monitoring of copper (II) ion, and presented in **Fig. S9**. The emission intensity of **HMAC**–Cu^{2+} complex was balanced within only 1 min, and it was proved that the extraordinarily rapid reaction between chemosensor **HMAC** and copper (II) ion was occurred. Moreover, the reversibility experiments were performed with EDTA, and the obtained results were presented in **Fig. S10**.

Computational DFT Studies

To support the experimental results, DFT calculations were performed on probe **HMAC** and **HMAC**–Cu^{2+}. Molecular orbital (MO) energies and figures of HOMO and LUMO levels are given in Fig. 6. The HOMO and LUMO of probe **HMAC** were spread over the molecules, but the electronic

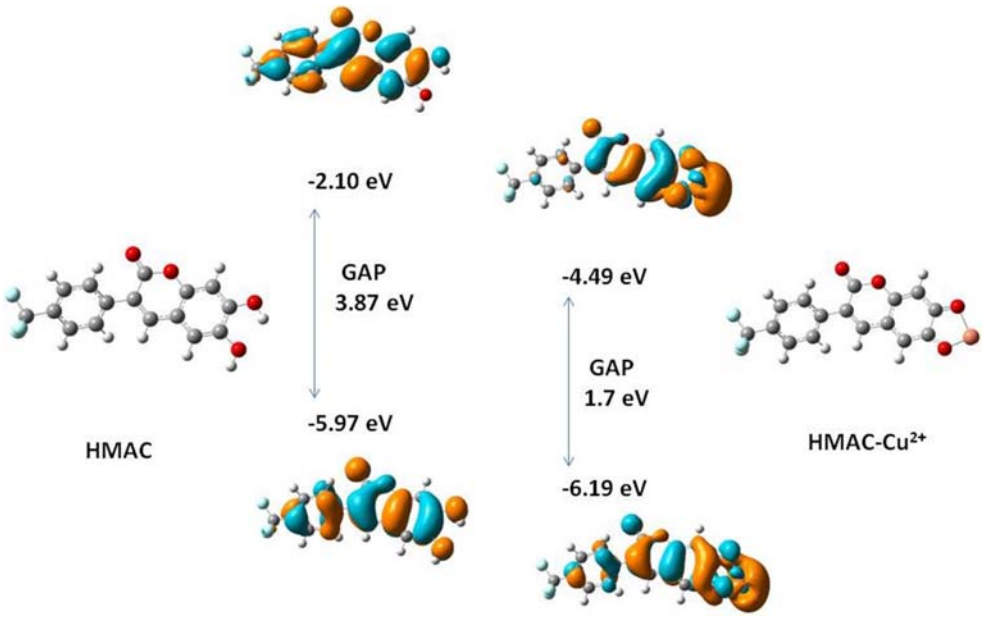


Fig. 6 Frontier molecular orbital profiles of probe **HMAC** and **HMAC**–Cu^{2+}complex

Table 1 The analysis of Cu^{2+} in various mineral and drinking water samples by probe **HMAC** and ICP–OES

	Cu (II) found (μmol L^{-1})		difference of the means	t test statistics (*df* = 2)		
	HMAC	ICP–OES		t Statistic	probability > |t|	
mineral water samples						
mineral water–A	1.18 ± 0.003	1.18 ± 0.001	0.0056	3.2095	0.0849	$t_{calculated} < t_{tabulated}$
mineral water–B	0.29 ± 0.006	0.30 ± 0.002	−0.0090	−2.0718	0.1740	$t_{calculated} < t_{tabulated}$
mineral water–C	1.23 ± 0.002	1.23 ± 0.001	−0.0016	−0.9351	0.4484	$t_{calculated} < t_{tabulated}$
mineral water–D	0.24 ± 0.003	0.25 ± 0.001	−0.0053	−2.0276	0.1797	$t_{calculated} < t_{tabulated}$
mineral water–E	0.55 ± 0.003	0.56 ± 0.004	−0.0059	−1.4388	0.2868	$t_{calculated} < t_{tabulated}$
drinking water samples						
drinking water–A	0.25 ± 0.003	0.25 ± 0.003	0.0048	2.6381	0.1186	$t_{calculated} < t_{tabulated}$
drinking water–B	0.50 ± 0.002	0.49 ± 0.001	0.0056	2.9099	0.1005	$t_{calculated} < t_{tabulated}$
drinking water–C	0.31 ± 0.007	0.31 ± 0.002	0.0045	1.3326	0.3141	$t_{calculated} < t_{tabulated}$
drinking water–D	0.20 ± 0.002	0.20 ± 0.001	−0.0027	−1.3361	0.3132	$t_{calculated} < t_{tabulated}$
drinking water–E	0.21 ± 0.004	0.21 ± 0.004	−0.0002	−0.0841	0.9406	$t_{calculated} < t_{tabulated}$
drinking water–F	0.10 ± 0.003	0.10 ± 0.001	0.0044	3.0072	0.0950	$t_{calculated} < t_{tabulated}$

† Null Hypothesis: mean1–mean2 = 0

†† Alternative Hypothesis: mean1–mean2 <> 0

††† At the 0.05 level, the difference of the population means is NOT significantly different with the test difference (0)

distribution weren't the same for the **HMAC**–Cu^{2+} complex. Although the LUMO of **HMAC**–Cu^{2+} complex was localized over the copper (II) ion and the coumarin moiety, HOMO of **HMAC**–Cu^{2+} complex was distributed around the molecules and copper (II) ion. The energy gap between HOMO to LUMO for probe **HMAC** and **HMAC**–Cu^{2+} is found as 3.87 and 1.17 eV. Probe **HMAC** provides a suitable molecular structure to coordinate with the copper (II) ion. After complexation, the interaction energy ($E_{int} = E_{complex} - E_{\mathbf{HMAC}} - E_{Cu}{}^{2+}$) is lowered by −11.94 eV (−275.348 kcal/mol), which proves

Table 2 Comparison of the performance of coumarin–based fluorescent probes reported in literature and probe **HMAC**

fluorescent probe	method performance			application	reference
	linear range	LOD	$\lambda_{ex}/\lambda_{em}$		
coumarin 7–yl picolinate based probe	0.1–0.9 μM	35 nM	325 nm/ 454 nm	tap water, deionized water	[29]
4,7–dihydroxy–3–aminocoumarin based probe	1.0–3.2 μM	256 nM	350 nm/ 475 nm	tap water, river water	[30]
CQP, (E)–ethyl–7–hydroxy–8–[[2–[2–(quinolin–8–yloxy)acetyl] hydrazono] methyl]–coumarin–3–carboxylate based probe	0.0–15.0 μM	52 nM	365 nm/ 410 nm	deionized water	[45]
7–diethylaminocoumarin–3–carbohydrazide (HCM) based probe	0.0–10.0 μM	210 nM	340 nm/ 458 nm	tap water, lake water	[46]
6,7–Dihydroxy–3–(4–(trifluoro)methylphenyl) coumarin based probe	0.0–30.0 μM	24.5 nM	365 nm/ 458 nm	drinking water, mineral water	this work

† LOD; limit of detection

the high affinity of probe **HMAC** towards copper (II) ions and the formation of a stable complex between probe **HMAC** and copper (II) ions. Thus, the obtained results indicate that the stabilized complex between probe **HMAC** and copper (II) ion has a lower HOMO–LUMO energy gap when compared to probe **HMAC**. This emission quenching response of probe **HMAC** was carried out due to the strong interaction between copper (II) ions and –OH as a result of the charge transfer process from the variation of electronic structure of probe **HMAC** [43, 44].

ICP–OES Analysis of Mineral and Drinking Water Samples

To prove the applicability of the probe **HMAC**, we performed analyses for copper (II) ion detection in various mineral and drinking water samples. The amount of copper (II) ion in tested samples was directly analyzed with a simple operation and quantitatively determined using the calibration curve. Also, a standard addition method was carried out (*final concentrations = 0.1* μM *and 0.2* μ*M*). The satisfactory recovery and relative standard deviation (RSD) values were obtained for all tested samples (**Table S2**). The recovery values of the method were obtained within a range of 95.48% to 106.01% for drinking waters and 96.18% to 109.20% for mineral waters, respectively. The results show the great potential and feasibility of the developed probe **HMAC** for the sensing of copper (II) ion in mineral and drinking water samples (**Table S2**).

The ICP–OES analyses were also performed (**Table S3**). Before ICP–OES measurements, the calibration curves were constructed by standard copper (II) ion solutions prepared in the concentrations from 10 to 1000 $\mu g.L^{-1}$. Besides, two different concentrations (10 and 20 $\mu g.L^{-1}$) of the standard solutions were spiked to the tested samples. The good agreements were obtained between the spiked and found amounts of copper (II) ion. The recovery values were between 91.05%–109.57% and the relative standard deviation (RSD) values were also obtained as lower (0.05%–2.78%) from ICP–OES measurements. The accuracy values of the probe **HMAC** and ICP–OES procedures were evaluated (Table 1). Moreover, the results were statistically evaluated employing *Student's t test* ($t_{calculated}$ *values* < $t_{tabulated}$ *values,* $d_f = 2$, *confidence level = 95%*). As a result, the results of probe **HMAC** and ICP–OES were in good agreement (Table 1). Therefore, the results of ICP–OES method prove the results of chemosensor **HMAC** for copper (II) ion sensing present in various mineral and drinking water samples.

Consequently, studies on the fluorescent chemosensor based on coumarin derivative for metal ion sensing in various drinking water samples are limited, and most of them are not related for copper (II) ion monitoring. The LOD for the chemosensor **HMAC** was determined to be less than 24.5 nM and it was below the current literature [29, 30, 45, 46] fluorescent probe's detection levels used for analysis of copper (II) ion in drinking water samples (Table 2). Overall, it is clear that the obtained results were accurate and had good recovery values, which confirm the reliability of the proposed assay, and could be applied to trace copper (II) ion sensing in real beverage samples quantitatively.

Conclusion

A fluorescent chemosensor based on coumarin derivative for copper (II) ion sensing with signal "turn–on–off" has been developed. The fabricated probe **HMAC** is a quite simple operation and offers a realistic potential for the trace copper (II) ion monitoring in the presence of other cations. The calibration plot of $1/(I–I_0)$ versus concentration of $1/Cu^{2+}$ was linear with a correlation coefficient of 0.9875. The LOD was found as 24.5 nM on the basis of $3\sigma/k$. The stoichiometry of the **HMAC–Cu^{2+}** complex was established by Job's method (1:1 ratio) and ESI–MS technique. In mineral and drinking water samples, copper (II) ions can be detected with excellent recovery values (95.48–109.20%). Furthermore, the ICP–OES results confirmed the results of **HMAC** for copper (II) ion sensing. Consequently, the presented approach is expected to have a great potential application for safety copper (II) monitoring in various drinking samples including water used in agriculture and environmental applications as well as in commercial distribution of beverages.

Acknowledgments The authors are grateful to the Research Fund of the TUBITAK for their support (for the synthesis of compound) with the project No–110 T652. The authors would also like to thank Scientific Research Project Center of Karamanoglu Mehmetbey University with the project 30–M–16 and for providing the financial support to use Gaussian 09 (Gaussian, Inc., Wallingford CT) program.

References

1. Wang S, Liu C, Li G, Sheng Y, Sun Y, Rui H, Zhang J, Xu J, Jiang D (2017) The triple roles of glutathione for a DNA-cleaving DNAzyme and development of a fluorescent glutathione/cu 2+ −dependent DNAzyme sensor for detection of cu 2+ in drinking water. ACS sensors 2:364–370. https://doi.org/10.1021/acssensors.6b00667
2. Yang S, Jiang W, Tang Y et al (2018) Sensitive fluorescent assay for copper(II) determination in aqueous solution using quercetin–cyclodextrin inclusion. RSC Adv 8:37828–37834. https://doi.org/10.1039/C8RA06754F
3. Gao J, Yin J, Tao Z, Liu Y, Lin X, Deng J, Wang S (2018) An ultrasensitive fluorescence sensor with simple operation for Cu2+

specific detection in drinking water. ACS Omega 3:3045–3050. https://doi.org/10.1021/acsomega.7b01497
4. Saleem M, Rafiq M, Hanif M, et al (2018) A brief review on fluorescent copper sensor based on conjugated organic dyes. Springer US
5. Hormozi-nezhad MR, Taghipour M (2015) An ultrasensitive and selective turn-offfluorescent nanoprobe for the detection of copper ions. Anal Methods 7:5067–5073. https://doi.org/10.1039/C5AY00766F
6. Wei F, Yu H, Hu M et al (2012) Manganese modified CdTe / CdS quantum dots as a highly selective probe to detect trace copper element in beer samples. Anal Methods 4:1438–1444. https://doi.org/10.1039/c2ay05794h
7. Liu H, Cui S, Shi F, Pu S (2019) A diarylethene based multi-functional sensor for fluorescent detection of Cd2+ and colorimetric detection of Cu2+. Dyes Pigments 161:34–43. https://doi.org/10.1016/j.dyepig.2018.09.030
8. Ngamdee K, Chaiendoo K, Saiyasombat C, Busayaporn W (2019) Highly selective circular dichroism sensor based on D - penicillamine / cysteamine cadmium sul fi de quantum dots for copper (II) ion detection. Spectrochim Acta Part A Mol Biomol Spectrosc 211:313–321. https://doi.org/10.1016/j.saa.2018.12.027
9. Robinson NJ, Winge DR (2010) Copper Metallochaperones. Annu Rev Biochem 10:537–562. https://doi.org/10.1146/annurev-biochem-030409-143539
10. Joo DH, Mok JS, Bae GH et al (2017) Colorimetric detection of Cu2+ and fluorescent detection of PO43− and S2− by a multifunctional Chemosensor. Ind Eng Chem Res 56:8399–8407. https://doi.org/10.1021/acs.iecr.7b01115
11. Liu Y, Liang P, Guo L (2005) Nanometer titanium dioxide immobilized on silica gel as sorbent for preconcentration of metal ions prior to their determination by inductively coupled plasma atomic emission spectrometry. Talanta 68:25–30. https://doi.org/10.1016/j.talanta.2005.04.035
12. Shi L, Jing C, Ma W et al (2013) Plasmon resonance scattering spectroscopy at the single- nanoparticle level: real-time monitoring of a click reaction ** Angewandte. Angew Commun:1–5. https://doi.org/10.1002/anie.201301930
13. Ghaedi M, Ahmadi F, Shokrollahi A (2007) Simultaneous preconcentration and determination of copper , nickel , cobalt and lead ions content by flame atomic absorption spectrometry. J Hazard Mater 142:272–278. https://doi.org/10.1016/j.jhazmat.2006.08.012
14. Kimmel DW, Leblanc G, Meschievitz ME, Cli DE (2012) Electrochemical sensors and biosensors. Anal Chem:685–707
15. Islamnezhad A, Mahmoodi N (2011) Potentiometric Cu2+−selective electrode with subnanomolar detection limit. Desalination 271:157–162. https://doi.org/10.1016/j.desal.2010.12.020
16. Feist B, Mikula B (2014) Preconcentration of heavy metals on activated carbon and their determination in fruits by inductively coupled plasma optical emission spectrometry. Food Chem 147:302–306. https://doi.org/10.1016/j.foodchem.2013.10.002
17. Karuk Elmas ŞN, Ozen F, Koran K, Yilmaz I (2017) Coumarin based highly selective off-on-off type novel fluorescent sensor for Cu2+ and S2− in aqueous solution. J Fluoresc 27:463–471. https://doi.org/10.1007/s10895-016-1972-3
18. Karuk Elmas ŞN, Ozen F, Koran K, Orhan A (2018) Selective and sensitive fl uorescent and colorimetric chemosensor for detection of CO 32- anions in aqueous solution and living cells. Talanta 188:614–622. https://doi.org/10.1016/j.talanta.2018.06.036
19. Karuk Elmas ŞN, Yilmaz I (2018) A turn off-on fluorescent Chemosensor for sequential determination of mercury and Biothiols. J Fluoresc 28:1451–1458
20. Jiao Y, Zhu B, Chen J, Duan X (2015) Fluorescent sensing of fluoride in cellular system. Theranostics 5:173–187. https://doi.org/10.7150/thno.9860
21. Aksuner N, Henden E, Yenigul B et al (2011) Highly sensitive sensing of zinc (II) by development and characterization of a PVC-based fluorescent chemical sensor. Spectrochim Acta Part A Mol Biomol Spectrosc 78:1133–1138. https://doi.org/10.1016/j.saa.2010.12.065
22. Aksuner N, Henden E, Yilmaz I, Cukurovali A (2010) Development of a highly sensitive and selective optical chemical sensor for the determination of zinc based on fluorescence quenching of a novel Schiff Base ligand. Sens Lett 8:684–689
23. Sonawane M, Sahoo SK, Singh J et al (2015) A lawsone azo dye-based fluorescent chemosensor for Cu2+ and its application in drug analysis. Inorganica Chim Acta 438:37–41. https://doi.org/10.1016/j.ica.2015.08.026
24. Sharma D, Kuba A, Thomas R et al (2016) An aqueous friendly chemosensor derived from vitamin B6 cofactor for colorimetric sensing of Cu2+ and fluorescent turn-off sensing of Fe3+. Spectrochim Acta - Part A Mol Biomol Spectrosc 153:393–396. https://doi.org/10.1016/j.saa.2015.08.051
25. Sahoo SK, Sharma D, Moirangthem A et al (2016) Pyridoxal derived chemosensor for chromogenic sensing of Cu2+ and fluorogenic sensing of Fe3+ in semi-aqueous medium. J Lumin 172:297–303. https://doi.org/10.1016/j.jlumin.2015.12.035
26. Venkatesan V, Selva Kumar R, Ashok Kumar SK, Sahoo SK (2019) Dual optical properties of new schiff base based on bisthiophene for sensing of Cu2+ in protic media. J Mol Struct 1198:126906. https://doi.org/10.1016/j.molstruc.2019.126906
27. Thangaraj A, Bhardwaj V, Sahoo SK (2019) A multi-analyte selective dansyl derivative for the fluorescence detection of cu(ii) and cysteine. Photochem Photobiol Sci 18:1533–1539. https://doi.org/10.1039/c9pp00080a
28. Wu X, Wang H, Yang S, Tian H, Liu Y, Sun B (2019) A novel coumarin-based fluorescent probe for sensitive detection of copper (II) in wine. Food Chem 284:23–27. https://doi.org/10.1016/j.foodchem.2019.01.090
29. Yan F, Bai Z, Chen Y et al (2018) Ratiometric fluorescent detection of copper ions using coumarin-functionalized carbon dots based on FRET. Sensors Actuators B Chem 275:86–94. https://doi.org/10.1016/j.snb.2018.08.034
30. Duan Y, Tang H, Guo Y et al (2014) The synthesis and study of the fluorescent probe for sensing cu 2 + based on a novel coumarin Schiff-base. Chinese Chem Lett 25:1082–1086. https://doi.org/10.1016/j.cclet.2014.05.001
31. Yuan L, Lin W, Yang Y et al (2011) Rational design of a highly reactive ratiometric fluorescent probe for cyanide. Org Lett 13:3730–3733. https://doi.org/10.1021/ol2013928
32. Krauter CM, Möhring J, Buckup T, Pernpointner M, Motzkus M (2013) Ultrafast branching in the excited state of coumarin and umbelliferone. Phys Chem Chem Phys 15:17846–17861. https://doi.org/10.1039/c3cp52719k
33. Feng Y, Yang Y, Wang Y et al (2019) Dual-functional colorimetric fluorescent probe for sequential Cu2+ and S2− detection in bio-imaging. Sensors Actuators B Chem 288:27–37. https://doi.org/10.1016/j.snb.2019.02.062
34. Buu-Hoi NP, Saint-Ruf G, Lobert B (1968) Oxygen Heterocycles. Part XIV. Hydroxylated 3-awl- and 3-Pyridyl- coumarins. J Chem Soc C 16:2069–2070
35. Ozen F, Tekin S, Koran K et al (2016) Synthesis , structural characterization , and in vitro anti-cancer activities of new phenylacrylonitrile derivatives. Appl Biol Chem 59:239–248. https://doi.org/10.1007/s13765-016-0163-x
36. Hay PJ, Wadt WR (1985) Ab initio effective core potentials for molecular calculations. Potentials for the transition metal atoms Sc to Hg J Chem Phys 82:270–283. https://doi.org/10.1063/1.448799

37. Lee C, Yang W, Parr RG (1988) Development of the Colle-Salvetti correlation-energy formula into a functional of the electron density. Phys Rev B 37:785–789. https://doi.org/10.1103/PhysRevB.37.785
38. Becke AD (1993) Becke's three parameter hybrid method using the LYP correlation functional. J Chem Phys 98:5648–5652
39. Frisch MJ, Trucks GW, Schlegel HB, et al (2009) Gaussian 09 Revision D.01
40. Dennington R, Keith TA, Millam JM (2009) GaussView Version 5
41. Mendil D, Karatas M, Tuzen M (2015) Separation and preconcentration of cu(II), Pb(II), Zn(II), Fe(III) and Cr(III) ions with coprecipitation method without carrier element and their determination in food and water samples. Food Chem 177:320–324. https://doi.org/10.1016/j.foodchem.2015.01.008
42. Yang S, Yin B, Xu L et al (2015) A natural quercetin-based fluorescent sensor for highly sensitive and selective detection of copper ions. Anal Methods 7:4546–4551. https://doi.org/10.1039/C5AY00375J
43. Angupillai S, Hwang J-Y, Lee J-Y et al (2015) Efficient rhodamine-thiosemicarbazide-based colorimetric/fluorescent "turn-on" chemodosimeters for the detection of Hg2+ in aqueous samples. Sensors Actuators B Chem 214:101–110. https://doi.org/10.1016/j.snb.2015.02.126
44. Hwang SM, Chae JB, Kim C (2018) A Phenanthroimidazole-based fluorescent turn-off Chemosensor for the selective detection of cu 2+ in aqueous media. Bull Kor Chem Soc 39:925–930. https://doi.org/10.1002/bkcs.11526
45. Zhou Z, Li N, Tong A (2011) A new coumarin-based fluorescence turn-on chemodosimeter for Cu2+ in water. Anal Chim Acta 702:81–86. https://doi.org/10.1016/j.aca.2011.06.041
46. Sheng JR, Feng F, Qiang Y et al (2008) A Coumarin-derived fluorescence Chemosensors selective for copper (II). Anal Lett 41:2203–2213. https://doi.org/10.1080/00032710802237673

Publisher's Note Springer Nature remains neutral with regard to jurisdictional claims in published maps and institutional affiliations.